66-2729
Translated from Russian

USSR STATE COMMITTEE ON THE USE OF ATOMIC ENERGY
NUCLEAR DATA INFORMATION CENTRE

Nuclear Physics Research in the USSR
(Volume of Abstracts)

No. 2

Edited by A.I. Abramov
and A. Savelev

Obninsk 1966

This volume presents the abstracts of work on the experimental or theoretical analysis of nuclear reactions induced by neutrons of energies up to ~20 MeV, and also of work on the fission of nuclei. It covers investigations carried out in certain institutes in the Soviet Union in the second half of 1965.

INSTITUTE OF PHYSICS AND ENERGETICS

(F.E.I.)

MULTIPARAMETER INVESTIGATION OF FRAGMENTS PRODUCED IN THE FISSION OF URANIUM-235 BY THERMAL NEUTRONS AND 5, 6 and 7 MeV NEUTRONS

V.G. Vorobeva, P.P. Dyachenko,
B.D. Kuzminov and M.Z. Tarasko

The authors measured the mass dependence of the total kinetic energy of the fragments accompanying the fission of ^{235}U induced by thermal neutrons and 5, 6 and 7 MeV neutrons.

The energy of the fission fragments was measured by silicon surface-barrier counters, and the measurements for thermal and fast neutrons were conducted in the same experimental conditions. The experimental value for the peak-to-valley ratio of the mass yield curve for the thermal neutron-induced fission of ^{235}U was 400:1; the width of this distribution was 34 atomic mass units. Within the limits of error of the experiments, the total kinetic energy of the fragments in the symmetrical fission of ^{235}U by 5, 6 and 7 MeV neutrons was the same, amounting to 157 $\pm$ 1 MeV. The comparable value for the thermal neutron-induced fission of ^{235}U was 152 $\pm$ 2 MeV which, after application of a correction for the contribution of spurious events, becomes 159 $\pm$ 4 MeV. It is concluded that the total kinetic energies of the fragments for thermal neutron-induced fission and that induced by 5, 6 and 7 MeV neutrons are in fact equal within the limit of error of the experiment.

DELAYED NEUTRONS AT THE FISSION THRESHOLD OF THORIUM-232

B.P. Maksyutenko

The author measured the relative delayed neutron yields for the fission of thorium-232 by neutrons from the reaction $T(p,n)He^3$ with a spectral peak half-width of ~500 keV. The results are given in Table I.

Table I

Half-life (sec)	Neutron energy (MeV)			
	1.6	1.9	2.2	2.6
55	1	1	1	1
24	1.47±0.08	1.89±0.06	1.93±0.04	2.04±0.03
15.5	2.67±0.11	2.36±0.08	2.26±0.06	1.95±0.04
5.2	2.47±0.15	3.71±0.11	3.41±0.08	3.23±0.08
2.2	12.8 ±0.3	8.57±20	7.98±0.14	5.83±0.13

Analysis of the energy dependence of the ^{232}Th fission cross-section shows that at the first step of the cross-section curve there is a considerable change in the group yield ratio.

ENERGY DEPENDENCE OF THE ANGULAR DISTRIBUTION OF FRAGMENTS FOR NEUTRON-INDUCED FISSION OF ^{233}U, ^{235}U and ^{239}Pu

V.G. Nesterov, G.N. Sminenkin and D.L. Shpak

Submitted to the Journal "Jadernaja fizika"

The authors report the results of measurements of the angular distribution of fragments for the neutron-induced fission of ^{233}U, ^{235}U and ^{239}Pu. The measurements for ^{233}U and ^{239}Pu were made in the neutron energy range 0.08 to 1.5 MeV, and for ^{235}U in the range 0.08 to 6 MeV. In the experiments they used a multiple ionization detector and a multichannel recorder for the fragments. This allowed them to measure the probability of fragment divergence at six angles to the incident neutron beam. The data are discussed in the light of present conceptions of the spectrum of the excited states of a compound nucleus.

The results of measurements of the angular distribution of the fragments $W(\vartheta)$ are given in Table II, $W(81^\circ)$ being taken as unity. The last column of the table gives the values for angular anisotropy $A = \frac{W(0^\circ)}{W(90^\circ)} - 1$ calculated by the least squares method on the assumption that $W(\vartheta)$ obeys the approximate relationship of statistical theory

$$W(\vartheta) \approx 1 + A \cos^2\vartheta, \qquad A > 0$$

Table II

Angular distributions of fission fragments

E ~ MeV	W(13°)	W(26°)	W(39°)	W(52.5°)	W(66.5°)	W(81°)	A
			U-233				
" 0,08 "	I,0I6±0,009	I,035±0,008	I,029±0,005	I,029±0,005	I,0I0±0,006	I,000±0,009	≈ 0,025
0,I7±0,05	I,053±0,008	I,034±0,005	I,028±0,005	I,024±0,004	I,0I5±0,005	I,000±0,008	0,04I±0,008
0,29±0,04	I,066±0,007	I,067±0,005	I,046±0,004	-	I,024±0,004	I,000±0,007	0,066±0,0I3
0,49±0,03	I,I0I±0,008	I,080±0,005	I,060±0,005	I,044±0,004	I,026±0,005	I,000±0,008	0,093±0,0I0
0,75±0,03	I,059±0,007	I,073±0,005	I,073±0,005	I,046±0,005	I,027±0,005	I,00I±0,005	0,09I±0,007
0,88±0,04	I,085±0,008	I,08I±0,008	I,060±0,005	I,044±0,005	I,0I5±0,005	I,000±0,008	0,095±0,009
0,98±0,04	I,I20±0,007	I,II7±0,005	I,089±0,004	I,059±0,004	I,036±0,005	I,000±0,007	0,I2I±0,009
I,26±0,04	I,II7±0,0I0	I,I0I±0,007	I,069±0,006	I,052±0,006	I,0I8±0,007	I,000±0,009	0,I23±0,0I2
			U-235				
" 0,08 "	0,950±0,009	0,970±0,007	0,984±0,006	0,993±0,006	0,996±0,006	I,000±0,008	- 0,06
0,I7±0,05	I,0I2±0,0I2	0,998±0,009	0,985±0,007	0,988±0,008	I,002±0,008	I,000±0,0I2	≈ 0
0,30±0,05	I,052±0,009	I,023±0,007	I,020±0,006	0,0I5±0,006	I,0I4±0,006	I,000±0,008	0,037±0,009
0,50±0,04	I,068±0,0II	I,046±0,007	I,025±0,007	I,0I5±0,006	I,0II±0,0II	I,000±0,0I0	0,059±0,0II
0,75±0,03	I,I09±0,0I0	I,099±0,0I0	I,078±0,007	I,054±0,008	I,030±0,0I0	I,000±0,0I0	0,II4±0,0I0
0,99±0,04	I,II9±0,006	I,095±0,006	I,057±0,005	I,042±0,005	I,027±0,006	I,000±0,007	0,II4±0,0I2
I,25±0,03	I,095±0,008	I,II2±0,006	I,080±0,005	I,059±0,005	I,028±0,005	I,000±0,007	0,III±0,0I4
I,5I±0,04	I,I27±0,0I3	I,I3I±0,009	I,075±0,008	I,039±0,008	I,0I6±0,008	I,000±0,0I3	0,I34±0,0I8
I,76±0,05	I,I57±0,008	I,I44±0,005	I,II8±0,005	I,068±0,004	I,0I6±0,005	I,000±0,007	0,I87±0,0I2
2,02±0,03	I,I85±0,009	I,I7I±0,006	I,II9±0,005	I,072±0,005	I,038±0,006	I,000±0,008	0,203±0,009
2,27±0,04	I,I78±0,006	I,I65±0,005	I,I2I±0,004	I,09I±0,004	I,038±0,005	I,000±0,005	0,I85±0,0I0
2,52±0,03	I,I75±0,009	I,I76±0,006	I,098±0,005	I,075±0,005	I,025±0,006	I,000±0,008	0,205±0,0I9

Continuation

2,76±0,04	I,I93±0,008	I,I54±0,005	I,I04±0,004	I,079±0,004	I,038±0,005	I,000±0,007	0,I83±0,008
3,0I±0,04	I,I78±0,007	I,I75±0,004	I,I43±0,004	I,09I±0,003	I,037±0,004	I,000±0,006	0,205±0,009
3,26±0,04	I,I82±0,008	I,I60±0,005	I,+3I±0,004	I,087±0,004	I,045±0,005	I,000±0,008	0,I84±0,009
3,54±0,03	I,I59±0,0II	I,I7I±0,007	-	I,I00±0,005	I,060±0,007	I,000±0,0II	0,I60±0,0I4
4,54±0,II	I,I55±0,008	I,I30±0,007	I,094±0,006	I,062±0,005	I,0I3±0,006	I,000±0,008	0,I72±0,008
5,20±0,I0	I,I43±0,006	I,I3I±0,005	I,09I±0,005	I,058±0,004	I,032±0,005	I,000±0,006	0,I52±0,006
5,52±0,09	I,I39±0,008	I,I24±0,006	I,086±0,006	I,064±0,004	I,005±0,006	I,000±0,008	0,I59±0,0I3
6,07±0,09	I,I76±0,006	I,I62±0,005	I,I06±0,005	I,080±0,004	I,032±0,005	I,000±0,006	0,I87±0,007
			Pu-239				
" 0,08 "	0,997±0,0II	0,988±0,008	0,997±0,007	0,99I±0,009	I,007±0,008	I,000±0,0I4	≈ 0
0,I7±0,05	I,026±0,0I0	I,025±0,007	I,025±0,006	I,0I8±0,006	I,0I4±0,006	I,000±0,008	0,025±0,0I0
0,29±0,05	I,072±0,0II	I,064±0,007	I,046±0,006	I,028±0,008	I,0II±0,007	I,000±0,0I2	0,079±0,0II
0,49±0,03	I,077±0,0I0	I,069±0,008	I,062±0,007	I,02I±0,009	I,0I6±0,009	I,000±0,0I2	0,086±0,0I0
0,75±0,03	I,075±0,006	I,068±0,004	I,050±0,004	I,029±0,004	0,998±0,008	I,000±0,006	0,089±0,006
0,90±0,03	I,048±0,006	I,06I±0,004	I,047±0,004	I,032±0,004	I,009±0,004	I,000±0,005	≈0,03
I,03±0,03	I,059±0,0I0	I,063±0,007	I,047±0,006	I,032±0,006	I,024±0,005	I,000±0,005	0,068±0,0I0
I,08±0,03	I,092±0,009	I,088±0,006	I,057±0,005	I,040±0,005	I,0I8±0,006	I,000±0,0I0	I,099±0,009
I,24±0,04	I,087±0,009	I,09I±0,007	I,069±0,006	I,046±0,006	I,028±0,007	I,000±0,0I0	0,094±0,009
I,50±0,04	I,I00±0,007	I,099±0,004	I,078±0,004	I,059±0,004	I,022±0,004	I,000±0,007	0,III±0,009

THE INTERACTION OF FAST NEUTRONS WITH MATTER

P.S. Otstavnov and V.E. Kolosov

The paper analyses the polarization of elastically scattered 3.4 MeV neutrons at an angle of 30° (lab), as a function of mass number and nuclear charge over a wide range of atomic weights. A calculation of polarization for the optical model of the nucleus is given.

There is qualitative agreement between the theoretical and the experimental data. A special characteristic observed in the dependence of polarization on nuclear charge is that the polarization is extreme for elements having integral values of $Z/3$. Possible ways of explaining this effect and defining it more accurately are indicated.

MEASUREMENT OF THE ABSORPTION CROSS-SECTIONS OF GADOLINIUM-154 AND -156

E.I. Gishanin, V.I. Lependin, L.Ya. Memelova et al. (?)

Samples of gadolinium oxide were irradiated in a reactor until equilibrium concentrations of the isotopes ^{155}Gd and ^{157}Gd were reached. The authors measured the reactor absorption cross-sections of the isotopes ^{154}Gd (σ_4 = 100 ± 20 b) and ^{156}Gd (σ_6 = 11.5 ± 7.2 b).

The required absorption cross-sections of ^{155}Gd and ^{157}Gd were obtained by calculation.

The quoted errors give the 98% confidence interval.

INELASTIC SCATTERING OF NEUTRONS ON NUCLEI OF CARBON, ALUMINIUM, TITANIUM, IRON AND BISMUTH

D.L. Broder, A.G. Dovbenko, V.E. Kolesov, A.I. Lashuk and I.P. Sadokhin

The radiative inelastic neutron scattering cross-section has been measured; for carbon, with neutrons of 15.6 and 16.0 MeV; for iron, with 6.26, 6.66, 6.86, 15.6 and 16.0 MeV neutrons; and for titanium,

with neutrons in the energy range from 1 to 3.2 MeV. The cross-sections for the excitation of levels in ^{27}Al and ^{209}Bi were measured in the energy range from 1 to 3.52 MeV. The experimental results are compared with theoretical calculations on the basis of statistical theory, the optical model of the nucleus having been used to calculate the neutron penetration factors. This comparison leads to the conclusion that the level scheme for the ^{209}Bi nucleus is of the form shown in Fig. 1.

In tables III and IV are given the radiative inelastic neutron scattering cross-sections for carbon, iron and titanium at various incident neutron energies.

Table III

Radiative inelastic neutron scattering cross-section for carbon and iron (in barns)

Element	En, MeV / Eγ, MeV	6.26	6.66	6.86	15.6	16.0
Fe	0.84	1.19	1.38	1.42	0.71	0.72
"	1.01	-	-	-	0.05	-
"	1.23	-	-	-	0.26	-
"	1.82	-	-	-	0.05	-
"	2.08	-	-	-	0.04	-
"	2.30	-	-	-	0.02	-
"	2.60	-	-	-	0.07	-
"	2.88	-	-	-	0.10	-
C	4.44	-	-	-	0.17	0.14

Table IV

Radiative inelastic neutron scattering cross-section for titanium

(differential and total)

Neutron energy MeV	Eγ = 0.99 MeV	Eγ = 1.38 MeV	Eγ = 1.56 MeV	Total
	b	mb	mb	b
1.10	0.14	-	-	0.14
1.20	0.36	-	-	0.36
1.30	0.32	-	-	0.32
1.41	0.43	50	-	0.48
1.50	0.48	33	-	0.52
1.61	0.53	31	-	0.56
1.70	0.61	32	-	0.65
1.81	0.76	61	-	0.82
1.90	0.59	50	-	0.64
2.01	0.65	77	58	0.79
2.10	0.68	51	61	0.79
2.21	0.77	91	70	0.93
2.30	0.67	47	71	0.79
2.41	0.75	62	68	0.88
2.50	0.74	30	59	0.83
2.61	0.85	99	40	0.99
2.70	0.93	85	71	1.09
2.81	0.84	122	79	1.04
3.01	0.87	189	83	1.14
3.21	0.78	152	75	1.50

The energy dependence of the inelastic neutron scattering cross-sections for ^{27}Al and ^{209}Bi are shown graphically. The theoretical dependence of the cross-sections on energy, found by the method of Hauser and Feshbach, is found to be in satisfactory agreement with the experimental data.

SPECTRA OF INELASTICALLY SCATTERED NEUTRONS WITH AN INITIAL ENERGY OF 14.1 MeV AND DENSITY OF THE NUCLEAR LEVELS

O.A. Salnikov, N.I. Fetisov, G.N. Lovchikov,
G.V. Kotelnikova, V.B. Anufrienko
and B.V. Devkin

The present paper on the measurement of the spectra of secondary neutrons from the nuclei of 14 elements (Be, Na, Mg, S, K, Ca, Sr, In, Sb, I, Cs, Ce, Ta, Hg) is a continuation of the work published in the first issue of this collection of abstracts (see No. 1, page 10, 1965*), which presents similar measurements for 23 elements.

Thus systematic data have been obtained on the secondary neutron spectra of 37 elements distributed approximately evenly, in terms of mass numbers A, from 9 to 209. These data warrant the following conclusions:

1. A description of most spectra of inelastically scattered neutrons in terms of nuclear temperature is quite feasible in the case of intermediate and heavy nuclides with an excitation energy of 10 MeV.

2. For 14.1 MeV neutrons the scattering accompanied by formation of a compound nucleus amounts to about 80%. Direct interaction plays a considerable part in the case of those neutrons which do not lose much energy during the scattering process.

3. The change observed in nuclear temperature with change in mass number and in excitation energies from 2 to 10 MeV is in good agreement with the Fermi gas model.

4. The level density is found to increase with increasing mass number, except for nuclei whose shells are almost filled, in which case there is a considerable reduction in level density. These results agree well, both qualitatively and quantitatively, with the values of the parameter α obtained from experimental data on the average distance between neutron resonances. There is agreement with the values of α obtained in the inelastic scattering of neutrons with an initial energy of 7 MeV.

---

*/ IAEA translation, INDSWG-120E.

RADIATIVE CAPTURE CROSS-SECTIONS FOR 30-170 keV NEUTRONS

V.N. Kononov, Yu.A. Stavissky, V.E. Kolesov,
A.G. Dovbenko, V.S. Nesterenko and V.I. Moroka

The authors have measured the radiative neutron capture cross-section for the nuclides ^{73}Ta, ^{74}W and ^{75}Re. The neutrons were obtained by the reaction $T(p,n)^{3}He$. The neutron energy was measured by the time-of-flight method with a resolution of 5-10%.

The experimentally determined energy dependence of the radiative neutron capture cross-section is compared with the predictions of the statistical theory of Hauser and Feshbach. This theory affords a satisfactory description of the experimental data. The average value of the radiation width $\overline{\Gamma}_{\gamma}$ and the average spacing between the levels $\overline{D}$, which are the parameters in the theory which correspond best with the experimental data, have proved to agree within the limits of error with the relevant values obtained from an analysis of isolated resonances.

EXCITATION FUNCTIONS AND YIELDS OF THE REACTIONS $^{181}Ta(d,2n)^{181}W$ and $^{181}Ta(p,n)^{181}W$

N.N. Krasnov and P.P. Dmitriev

The authors have experimentally determined the excitation functions of the reactions $^{181}Ta(d,2n)^{181}W$ and $^{181}Ta(p,n)^{181}W$, and the dependence of the ^{181}W yield on the deuteron and proton energy up to E_d = 21 MeV and E_p = 22 MeV. The overall error of measurement in the cross-sections of the reactions for obtaining ^{181}W is ±15%. The ^{181}W yield was measured during irradiation of targets in a cyclotron under conditions of industrial isotope production. The results obtained are compared with the data from other studies.

Table V

Deuteron energy MeV	Cross-section of the reaction $^{181}Ta(d,2n)^{181}W$, mb	Yield for a thick target, μCi/μA.h	Proton energy MeV	Cross-section of the reaction $^{181}Ta(p,n)^{181}W$, mb	Yield for a thick target, μCi/μA.h
6	10	-	6	2	-
8	165	0.1	8	45	0.05
10	565	1.2	10	98	0.85
12	650	3.3	12	65	2
14	575	6	14	30	2.85
16	440	8.4	16	18	3.1
18	330	10.5	18	9	3.2
20	250	11.9	20	7	3.22
21	215	12.5	22	5	3.25

YIELDS OF NUCLEAR REACTIONS IN THE CYCLOTRON PRODUCTION OF MANGANESE-54

N.N. Krasnov and P.P. Dmitriev

The authors have determined experimentally the dependence of ^{54}Mn yield on particle energy (for a thick target), upon irradiation of chromium and manganese with 22 MeV protons, chromium and iron with 21 MeV deuterons and vanadium and chromium with 42 MeV α-particles. The overall error of measurement for the ^{54}Mn yields was ±15%. The results obtained are compared with data from the work of other authors.

Table VI

Particle energy MeV	^{54}Mn yield in μCi/μA.h for the various methods of production					
	Cr+p	Mn+p	Cr+d	Fe+d	V+α	Cr+α
2	-	-	0.02	-	-	-
4	-	-	0.12	0.01	-	-
6	0.01	-	0.26	0.1	-	-
8	0.05	-	0.44	0.3	0.1	-
10	0.12	0.1	0.67	0.6	0.15	-
12	0.21	0.2	0.92	1	0.25	-
14	0.29	1	1.16	1.4	0.6	-
16	0.35	4.4	1.4	1.8	0.8	0.1
18	0.39	9.9	1.63	2.2	1.15	0.15
20	0.42	15.6	1.86	2.6	1.3	0.2
22	0.45	21	2	2.78	1.4	0.3
24					1.55	0.55
28					1.6	1.75
32					1.65	3.1
36					1.65	4.4
40					1.65	5.5
42					1.7	5.8

I. V. KURCHATOV ATOMIC ENERGY INSTITUTE

FISSION CROSS-SECTIONS OF ^{238}Pu AND ^{241}Am FOR MONOCHROMATIC RESONANCE NEUTRONS

F.F. Gerasimov

The fission cross-section of ^{238}Pu was measured in the energy range 0.02-400 eV, and that of ^{241}Am in the range 0.02-50 eV. Five resonances were detected in the fission cross-section of ^{238}Pu in the energy range up to 100 eV.

The fission widths were determined for the first three resonances. In view of the absence of information in the literature on the neutron widths of the other resonances of ^{238}Pu, only the $\sigma_{of} \times \Gamma$ values were determined for them; these are given in Table VII.

Table VII

Resonance parameters of ^{238}Pu

Eo (eV)	$\sigma_{of} \Gamma$ (b.eV)	Γ_f (MeV)
2.89	$(0.76 \pm 0.15) \cdot 10^{-2}$	0.005 ± 0.002
9.98	7.8 ± 0.6	0.11 ± 0.06
18.56	14.0 ± 1.0	0.11 ± 0.06
70.3	6.3 ± 0.7	
83.2	20.0 ± 1.8	

From the fission cross-section of ^{241}Am, the Γ_f / Γ values were determined for 13 levels at energies below 15 eV (See Table VIII).

Table VIII

Γ_f/Γ for ^{241}Am

Eo (eV)	$(\Gamma_f/\Gamma).10^2$
0.306	0.76±0.12
0.575	0.34±0.05
1.27	0.74±0.07
1.68	-
1.93	0.16±0.03
2.36	0.45±0.15
2.60	0.32±0.10
4.00	0.36±0.09
4.40	-
5.05	0.55±0.25
5.48	1.01±0.10
6.20	0.51±0.25
9.30	0.59±0.25
10.05	3.2 ±0.6
15.04	0.85±0.20

Fig. 2 shows the energy dependence of the fission cross-section of ^{238}Pu, while that for ^{241}Am is illustrated in Figs. 3 and 4.

The measurements of the cross-section for fission induced by monochromatic neutrons were carried out by the time-of-flight method using a linear electron accelerator from the I.V. Kurchatov Atomic Energy Institute.

INSTITUTE OF PHYSICS

UKRAINIAN ACADEMY OF SCIENCES

NEUTRON CROSS-SECTIONS OF ZrT_2 AND $ZrD_{1.6}$

V.P. Vertebny, M.F. Vlasov, A.L. Kirilyuk,
V.V. Koloty, M.V. Pasechnik and V.A. Stepanenko

Paper to the XVI Annual Conference on
Nuclear Spectroscopy and Structure of the Atomic Nucleus
Moscow, 1966

This work was done with mechanical neutron choppers and in accordance with the transmission method. The total neutron cross-sections of the zirconium hydrides ZrT_2 and $ZrD_{1.6}$ were measured with resolutions of 1.8, 3.6 and 6.4 μs/m, while their total neutron scattering cross-sections were measured in 4π geometry relative to vanadium and lead, with resolutions of 12 and 24 μs/m.

The experiment was set up in conjunction with the problem of the existence of a bound state of ^4H: the scattering amplitude close to zero bombarding energy was sensitive to the position of the bound state in the potential well.

The fact that there is no energy dependence of the scattering cross-section of tritium in the energy range 0.1-0 MeV contradicts the idea that there is a bound state of ^4H.

The total scattering cross-section of bound tritium in these measurements is determined as 1.30 ± 0.03 b (only statistical error is taken into account; the systematic error does not exceed 20%).

ELASTIC AND INELASTIC SCATTERING OF MEDIUM-ENERGY NEUTRONS: THE ELASTIC SCATTERING OF 0.8-MeV NEUTRONS BY ATOMIC NUCLEI - AN ANALYSIS IN TERMS OF THE OPTICAL MODEL OF THE NUCLEUS

M.V. Pasechnik, I.A. Korzh, I.E. Kashuba and I.A. Totsky

Paper to the Antwerp Conference, 1965*/

The work analyses, on the basis of the optical model of the nucleus, data on the angular distributions of neutrons with an initial energy of 0.8 MeV scattered by Na, Mg, Al, Si, Cr, Fe, Ni, Cu, Zn, Se, Zr, Mo, Cd, Sn, Sb, Te, Ba, W, Hg, Pb, Bi and U. In the calculations use is made of a diffuse edge potential, surface absorption and a spin-orbit term. The parameters of the model giving the best agreement between the calculated differential cross-sections and the experimental values were found for each element.

SCATTERING OF MEDIUM-ENERGY NEUTRONS

M.V. Pasechnik, I.A. Korzh and I.A. Totsky

Submitted to the journal "Atomnaja Energija"

The paper presents a brief review of work carried out on the electrostatic generator at the Physics Institute of the Ukrainian SSR Academy of Sciences.

It gives the results of research on the inelastic scattering of neutrons with energies of 0.8 MeV, 2.5 MeV, 3.3 MeV, 3.6 MeV and 4.1 MeV on C, Na, Mg, Al, P, S, Cl, Ca, Cr, Fe, Co, Ni, Cu, Zn, Se, Zr, Mo, Ag, Cd, Sn, Sb, Te, I, Ba, W, Hg, Pb, Bi and U.

These investigations have made it possible to determine the effect of the nuclear shells in the inelastic scattering of neutrons. The paper also gives the results of angular distribution measurements of elastically scattered neutrons with energies of 0.3 MeV, 0.5 MeV, 0.65 MeV and 0.8 MeV on C, Na, Mg, Al, Si, K, Cr, Fe, Ni, Cu, Zn, Se, Zr, Mo, Ag, Cd, Sn, Sb, Te, Ba, W, Hg, Pb, Bi and U. The results of the angular distribution measurements are analysed on the basis of the optical model of the nucleus.

---

*/ International Conference on the Study of Nuclear Structure with Neutrons, Antwerp, 23 July 1965.

MEASUREMENT OF THE ANGULAR DISTRIBUTIONS OF 0.3, 0.5 AND 0.8-MeV NEUTRONS ELASTICALLY SCATTERED ON TITANIUM AND COBALT NUCLEI

I.A. Korzh, V.A. Mishchenko, M.V. Pasechnik, N.M. Pravdivy, V.P. Prikhodko, N.T. Sklyar and I.A. Totsky

Submitted to the Ukrainian Journal of Physics

The paper gives the results of measurements of the angular distributions of elastically scattered neutrons with energies of 0.3 and 0.5 MeV on titanium nuclei, and with energies of 0.5 and 0.8 MeV on cobalt nuclei. The results of the differential elastic scattering cross-section measurements are compared with calculation based on the optical model of the nucleus using a diffuse-edge potential, surface absorption and a spin-orbit term.

ANALYSIS OF THE ELASTIC SCATTERING OF POLARIZED 3.4-MeV NEUTRONS BY S, Cu, Zn AND Zr, ACCORDING TO THE OPTICAL MODEL OF THE NUCLEUS

I.E. Kashuba, I.A. Korzh and B.D. Kozin

Paper to the XVI Annual Conference on Nuclear Spectroscopy and the Structure of the Atomic Nucleus

The paper analyses, in terms of the optical model, the experimental data available in the literature on differential elastic neutron scattering cross-sections and on the polarization occurring in the elastic scattering of 3.4-MeV neutrons by S, Cu, Zn and Zr. In calculations based on the Schrödinger single-particle equation, the authors used a local optical diffuse-edge potential and surface absorption. The paper also gives a set of model parameters obtained by adjusting the theoretical results to the experimental results by the χ^2 method.

INVESTIGATION OF THE INELASTIC SCATTERING OF SLOW NEUTRONS ON POLYETHYLENE

P.G. Ivanitsky and V.T. Krotenko

Submitted to the journal "Atomnaja Energija"

The horizontal channel of the VVR-M (water-cooled and water-moderated) reactor of the Institute of Physics of the Ukrainian SSR Academy of Sciences was used in conjunction with the time-of-flight method to measure the spectra of slow neutrons inelastically scattered at different angles (15°, 30°, 60°, 90°, 120°) on polyethylene with different energies of the incident neutrons (15.4 meV, 25.5 meV, 49.4 meV, 98.8 meV, 136.1 meV, 193.2 meV and 317 meV). Analysis of the experimental data gave absolute values of the doubly differential cross-sections for the scattering of neutrons on polyethylene. An M-20 computer was used to calculate, on the basis of these cross-sections, the average characteristics of neutron scattering on polyethylene (mean energy of scattered neutrons and its dependence on incident neutron energy and scattering angle, mean energy loss in scattering, logarithmic decrement, average cosine of the scattering angle $\bar{\mu}$ etc.). The results of the calculations are given in Table IX.

The scattering law $S(\alpha,\beta)$ and the generalized frequency spectrum $\nu P(\beta)$ for polyethylene were found by the method of Egelstaff.

Table IX

Average characteristics of the scattering of slow neutrons on polyethylene. $T = 23^\circ C$

1	2	3	4	5	6	7
E meV	$\vartheta = 15^\circ$	$\vartheta = 30^\circ$	$\vartheta = 60^\circ$	$\vartheta = 90^\circ$	$\vartheta = 120^\circ$	Average of 2–6
			$\bar{E}'$			
15.4	20.6	20.2	20.6	22.0	22.4	21.1
25.5	30.8	29.1	30.5	31.2	31.3	30.7
49.4	52.9	51.7	51.8	50.6	50.2	51.0
98.8	101.1	100.1	96.6	90.0	83.4	92.2
136.1	134.3	132.1	124.1	112.9	104.9	117.5
193.2	178.9	177.5	160.8	153.3	134.6	157.9
317	294	294	238.1	208.6	192.5	230.1

1	2	3	4	5	6	7
		$\bar{\varepsilon} = \bar{E}' - \bar{E}$ meV				
15.4	-	4.84	5.16	6.56	6.98	5.74
25.5	-	3.66	4.98	5.67	5.75	5.10
49.4	3.46	2.32	2.35	1.24	0.75	1.61
98.8	2.26	1.31	-2.21	-8.85	-15.45	-6.57
136.1	-1.78	-3.99	-11.81	-23.19	-31.18	-18.61
193.2	-16.02	-15.48	-34.16	-41.67	-60.37	-37.07
317	-23.51	-22.19	-78.88	-108.4	-124.5	-86.86
		$\bar{\xi} = \ln \bar{E/E'}$				
15.4	-0.203	-0.164	-0.194	-0.245	-0.249	-0.267
25.5	-0.112	-0.091	-0.113	-0.098	-0.080	-0.102
49.4	-0.033	-0.010	0.016	0.059	0.092	0.032
98.8	0.008	0.021	0.082	0.170	0.285	0.122
136.1	0.064	0.073	0.177	0.299	0.390	0.207
193.2	0.176	0.196	0.311	0.394	0.534	0.332
317	0.277	0.241	0.467	0.619	0.774	0.534
		$\sigma(\vartheta) = \int \frac{d^2\sigma}{d\Omega\, dE'} dE'$ b/ster.				$\bar{\mu} = \overline{\cos\vartheta}$
15.4	15.7	12.9	12.3	11.7	9.5	0.168
25.5	13.4	11.7	10.1	10.3	7.8	0.185
49.4	13.5	11.3	9.1	8.3	6.0	0.222
98.8	12.2	9.2	6.8	5.6	3.8	0.252
136.1	13.4	9.4	6.7	5.1	3.6	0.261
193.2	13.2	10.2	5.9	3.9	2.7	-
317	10.5	8.7	4.9	3.3	3.1	0.264

V. G. KHLOPIN RADIUM INSTITUTE

KINETIC ENERGIES OF FRAGMENT PAIRS OCCURRING IN THE FISSION OF ^{233}U, ^{235}U AND ^{238}U BY 12-MeV DEUTERONS

Yu.A. Selitsky, S.M. Soloviev and V.P. Eismont

Using semiconductor detectors the authors measured the energies of fragment pairs occurring in the fission of uranium isotopes by 12.1-MeV deuterons. All the targets had a thickness of about 100 $\mu g\ cm^{-2}$ and were deposited on aluminium film having a thickness of 60 $\mu g\ cm^{-2}$. The fission fragment energies were measured at an angle of 90° to the deuteron beam and of 45° to the target plane. From measurements of some 20 000 fission events for each isotope, contour diagrams were obtained. These serve as a basis for discussing the mass distribution of the fragments, the mean kinetic energies, and the energy dispersions for fragments of given mass.

The yield curves (peak-to-valley ratio) show that the excitation energies of the compound nuclei are close to 20 MeV, which corresponds to complete deuteron capture. All the kinetic energy characteristics therefore refer to the fission of ^{240}Np, ^{237}Np and ^{235}Np (corresponding respectively to ^{238}U, ^{235}U and ^{233}U). From analysis of the measured kinetic energies and dispersions, and from comparison with other published data, it appears that:

(a) At intermediate excitation energies the shell structure of the fragments is much less pronounced than at low energies.

(b) The energy of fragments produced by symmetrical fission has a unique dependence on the coulomb factor $Z^2/A^{1/3}$ for light and heavy nuclei.

(c) The dispersions of the kinetic energies of fragments produced by symmetrical fission of different nuclei at identical excitation energies (of the order of 20 MeV) increases linearly as Z^2/A.

These phenomena can be explained simply in terms of a model based on two types of fission, although that does not exclude the possibility of interpreting them in terms of shell effects in the fragments.

FISSION OF ^{226}Ra BY 12-MeV DEUTERONS AND THE SHAPES OF THE FISSION-FRAGMENT KINETIC ENERGY DISTRIBUTIONS

Yu.A. Nemilov, Yu. A. Selitsky,
S.M. Soloviev and V.P. Eismont

Using semiconductor detectors and working with the Lenin University cyclotron, the authors measured the kinetic energies of fragment pairs arising in the fission of ^{226}Ra by 12.1 MeV deuterons.

About 15 000 fragment pairs were recorded. Fig. 5 shows the distributions of fragment yield, of total kinetic energy and of its dispersion, as a function of the mass of the heavy fragment. Of greatest interest are the shapes of the kinetic energy distributions for a number of mass ratios shown in Fig. 6. It can be seen that the shape is not symmetrical and that it changes with varying fragment mass ratio. As shown in Fig. 6, the distributions can be separated into two Gaussian curves 15 MeV apart and with a constant half-width corresponding to symmetrical fission.

The asymmetry found by the authors could be associated with the superposition of ^{228}Ac fissions arising from excitations at 20 MeV and fissions of ^{227}Ac formed after neutron emission. Estimates made by the authors show that approximately the same number of fissions occur for both nuclei in this experiment. If this superposition causes the asymmetry, then it must be assumed that the mean kinetic energies of fragments produced by ^{227}Ac fission (which appears to be mainly assymetrical) is approximately 15 MeV greater than in the case of ^{228}Ac fission (which appears to be mainly symmetrical). Proof that such changes do occur with changing excitation energy must include measurements at lower energies of the fissioning nuclei, when there is no superposition.

The asymmetry may also be explained by the hypothesis that there are two types of fission. From the area under each of the Caussian curves one can find, for the different fragment masses, the ratio of symmetrical to asymmetrical fission, and thus determine the remaining fission characteristics: mean kinetic energy and dispersion as a function of fragment mass. The curves obtained in this way are shown in Fig. 5 as dotted lines.

STUDY OF GAMMA SPECTRA AND IDENTIFICATION OF NEUTRON-DEFICIENT OSMIUM ISOTOPES

B.N. Belyaev, B.A. Gvozdev, V.I. Gudov,
A.V. Kalyamin and L.M. Krizhansky

Using a scintillation gamma spectrometer the authors investigated the gamma radiation of neutron-deficient osmium isotopes. The osmium isotopes were obtained from the reaction Yb(^{12}C, xn)Os by bombarding ytterbium targets enriched in ^{172}Yb, ^{174}Yb and ^{176}Yb with 80-MeV ^{12}C ions and from the reaction Tm(^{15}N,xn)Os by bombarding thulium targets enriched in ^{169}Tm with 100-MeV ^{15}N ions. The osmium was separated from the irradiated targets by radiochemical methods.

By using ytterbium targets enriched in certain isotopes, bombarding them with heavy ions and extracting the osmium decay products, it was possible to identify the isotopes ^{180}Os and ^{181}Os.

A half-life $T_{1/2}$ = 21 min. and the following gamma lines and relative intensities were found for ^{180}Os:

Table X

E_γ keV	Relative intensity
105	0.6
165	0.6
230	5.3
310	1.3
400	0.8
510	10.5
615	1.5
880	100
1050	0.5
1300	2.5
1550 ?	
2000 ?	

This study is connected with the decay chain $^{180}Os \xrightarrow{21\ min} {}^{180}Re \xrightarrow{2.4\ min}$. A half-life $T_{1/2}$ = 2.5 hr and the following gamma lines and relative intensities were found for ^{181}Os.

Table XI

E_γ keV	Relative intensity
130	140
250	250
815	270

It was found that in the decay of ^{181}Os approximately 1.5 gamma quanta were emitted per disintegration. It was also found that the 130-keV and 250-keV gamma lines coincided.

A. F. IOFFE INSTITUTE OF PHYSICS AND TECHNOLOGY

ISOSPIN DEPENDENCE OF NUCLEAR POTENTIAL FROM DATA ON THE TOTAL NEUTRON CROSS-SECTIONS OF ISOTOPES

Yu.V. Dukarevich, A.N. Dyumin and D.M. Kaminker

Paper presented at XVI Annual Conference on Nuclear Spectroscopy and Structure

The total neutron cross-sections (σ_t) were measured for nickel-58, 60, 62 and 64; zinc-64, 66, 67, 68 and 70; silver-107 and 109; cadmium-106, 108, 110-114, 116; indium-115; tin-112, 116-120, 122, 124; antimony-121 and 123; and tellurium-122, 124, 125, 126, 128 and 130 at a neutron energy of 14.2 MeV. It was found that the behaviour of the cross-section for the chains of isotopes of the measured elements differs from the behaviour of σ_t as a function of the atomic weight in the case of elements of natural isotopic composition and differs in various mass regions.

The total cross-sections for the selected nuclides are not equal; they are larger for isobars that have an excess of neutrons than for neutron-deficient nuclides in the vicinity of Cd-Te, and smaller in the vicinity of Ni-Zn.

An analysis was made of the data using the optical model with surface absorption. It is shown that, in order to achieve agreement between the calculated behaviour of the cross-sections and their behaviour as found by experiment, it is necessary to introduce a dependence of the depths of the real and imaginary parts of the potential on the asymmetry parameter of the nucleus, $\alpha = \frac{N-Z}{A}$. Using the surface absorption model, values were obtained for the real and imaginary parts of the isospin term of the potential:

$$V_1 = -(17 \pm 2) \text{ MeV} \qquad W = -(26 \pm 9) \text{ MeV}$$

On the basis of an optical model analysis of the total cross-sections, reaction cross-sections and differential cross-sections for elements of natural isotopic composition the authors suggest that a significant contribution is made by volume absorption at the energies considered. A table of cross-sections is attached.

Table XII

No.	Isotope	Weight of sample (g)	Enrichment of sample (%)	Total cross-section σ_t (barns)	No.	Isotope	Weight of sample (g)	Enrichment of sample (%)	Total cross-section σ_t (barns)
1	Ni58	6.51	96.8	2.701 ± 0.008	21	Sn112	3.62	66.2	4.41 ± 0.03
2	60	6.94	95.4	2.744 ± 0.009	22	116	0.48	86.2	4.43 ± 0.03
3	62	7.17	86.5	2.796 ± 0.010	23	117	0.98	84.8	4.64 ± 0.05
4	64	7.30	76.9	2.834 ± 0.010	24	118	0.87	85.0	4.75 ± 0.07
5	Zn64	5.59	91.6	2.965 ± 0.010	25	119	0.96	50.7	4.46 ± 0.10
6	66	5.66	89.2	3.011 ± 0.010	26	120	1.96	94.1	4.66 ± 0.04
7	67	5.81	30.9	2.99 ± 0.03	27	122	0.99	83.3	4.69 ± 0.04
8	68	5.52	92.3	3.051 ± 0.010	28	124	0.96	92.6	4.71 ± 0.06
9	70	5.64	44.9	3.116 ± 0.018	29	Sb121	4.98	97.5	4.66 ± 0.02
10	Ag107	5.0		4.34 ± 0.03	30	123	5.04		4.68 ± 0.03
11	109	5.0	98.8	4.38 ± 0.02	31	Te122	1.83	72.2	4.65 ± 0.04
12	Cd106	5.00	22.1	4.29 ± 0.07	32	124	1.73	54.8	4.60 ± 0.05
13	108	4.90	20.2	4.33 ± 0.07	33	125	2.34	52.3	4.69 ± 0.04
14	110	2.40	65.0	4.34 ± 0.04	34	126	2.42	84.1	4.73 ± 0.02
15	111	1.20	61.3	4.44 ± 0.04	35	128	1.42	92.6	4.76 ± 0.03
16	112	4.90	69.6	4.53 ± 0.03	36	130	4.74	94.2	4.81 ± 0.02
17	113	4.90	55.5	4.50 ± 0.03	37	Pb204	4.79	36.6	5.43 ± 0.06
18	114	5.78	90.6	4.54 ± 0.02	38	206	6.22	68.5	5.37 ± 0.04
19	116	4.95	72.4	4.56 ± 0.03	39	207	4.03	56.7	5.30 ± 0.05
20	In115	4.90		4.54 ± 0.02	40	208	3.25	94.8	5.26 ± 0.04
					41	Bi209		100	5.33 ± 0.04

ISOMERISM OF FISSION-FRAGMENT NUCLEI

L.A. Popeko, G.V. Valsky, G.A. Petrov
and D.M. Kaminker

Paper presented at XVI Annual Conference on Nuclear
Spectroscopy and Structure

The authors measured the spectra of gamma quanta from fragments with a neutron excess formed in the fission of ^{235}U by thermal neutrons, between 10 and 100 ns after fission. They found that:

1. The lifetimes of the excited states of fission-fragment nuclei in the energy range 30-800 keV were $\tau_{light} = 32 \pm 5$ ns for the light fragments and $\tau_{heavy} = 28 \pm 3$ ns for the heavy fragments.

2. In the gamma ray spectra a number of lines were obtained with the following energies and yields:

Table XIII

Light fragments		Heavy fragments	
E_γ (keV)	Intensity per 100 fissions	E_γ (keV)	Intensity per 100 fissions
85 ± 5	0.7 ± 0.4	30 ± 5	1.7
115 ± 10	0.5 ± 0.5	80 ± 5	1.0 ± 0.4
140 ± 5	1.8 ± 0.8	110 ± 5	1.1 ± 0.4
165 ± 10	1.0 ± 0.5	140 ± 5	0.7 ± 0.4
210 ± 8	2.3 ± 0.4	175 ± 10	0.4 ± 0.2
320 ± 10	0.5 ± 0.2	310 ± 10	1.4 ± 0.2
365 ± 10	2.3 ± 0.2		

3. Analysis of the mass yield curve for the fission fragments showed that the delayed gamma radiation is emitted mainly in the following mass intervals: A = 88-93, 93-100, 105-110, 128-135 and 145-160.

4. The mass yield curves obtained for the fragments coincided with the delayed gamma radiation of 100-185 keV and 185-250 keV.

The experimental results are discussed in terms of the theory of deformed nuclei.

KINETIC ENERGIES OF FRAGMENTS PRODUCED IN THERMAL NEUTRON-INDUCED FISSION

G.Z. Borukhovich and G.A. Petrov

Submitted to "Jadernaja fizika"

Using two surface-barrier counters (area - 8 cm^2) the authors measured the kinetic energies of fragments originating with fission induced by thermal neutrons. The ^{241}Pu target (diameter - 1 cm) contained 1 μg of ^{241}Pu deposited on an aluminium oxide tray. The total kinetic energy for different mass ratios was determined to within $\pm$ 2 MeV.

The dependence of total kinetic energy on the mass ratios of the fragments is shown in Fig. 7.

CROSS-SECTIONS OF PHOTONEUTRON REACTIONS IN ^7Li

E.B. Bazhanov, A.P. Komar and A.V. Kulikov

Submitted to "Phys. Letters"

By recording delayed neutrons with BF_3 counters the authors obtained a curve for the cross-sections of photoneutron reactions in ^7Li from the γ,n-reaction threshold to E_γ = 50 MeV.

It was found that the differential cross-section curve has a number of maxima, i.e. at the following energies: 11.5, 13.5, 15.0, 16.3, 17.8, 19.5, 22.0, 23.7, 26.0, 28.3, 30.3, 33.0, 34.7, (41.0) and (46.5) MeV. The data obtained are in satisfactory agreement with the results of other experiments on the photodisintegration of ^7Li. The authors note the importance of the multiparticle decay channels of the excited ^7Li nucleus.

SCIENTIFIC RESEARCH INSTITUTE FOR ATOMIC REACTORS

MEAN SPECTRA OF NEUTRONS FORMED IN THE BINARY AND TERNARY FISSION OF ^{235}U INDUCED BY THERMAL NEUTRONS

V.N. Nefedov, N.I. Kroshkin,
V.P. Kharin and A.K. Melnikov

Using the time-of-flight method the authors measured the spectra, averaged over angle, of prompt neutrons originating with the binary and ternary fission of ^{235}U induced by thermal neutrons. The measurements showed that the spectra for binary and ternary fission are identical in shape. The mean energy (~1.8 MeV) of the neutrons formed in ternary fission was somewhat less than that of the neutrons from binary fission (~1.98 MeV). The average number of neutrons emitted with each ternary fission event was found; $\nu_{3f} = 1.75 \pm 0.08$.

The ratio of ternary to binary fission neutron yield was $\nu_{3f}/\nu_{2f} \simeq 0.71$.

If approximately 7.5 gamma quanta are emitted with each ^{235}U binary fission event, then about 6.6 gamma quanta are emitted with each ternary fission event. The gamma spectrum for ternary fission is somewhat harder than that for binary fission.

PAPERS RECEIVED DURING 1965 AT THE NUCLEAR DATA INFORMATION CENTRE (NDIC) FROM THE JOINT INSTITUTE FOR NUCLEAR RESEARCH, DUBNA

NEUTRON RESONANCES OF YTTERBIUM ISOTOPES

Van-Nai-yan, E.N. Karzhavina, A.B. Popov,
Yu.S. Yazvitsky and Yao-Tchi-chuan
JINR Preprint P-2158, Dubna, 1965

Using the slow-neutron spectrometer at the Neutron Physics Laboratory of the Joint Institute for Nuclear Research the authors measured the transmission of neutrons by natural ytterbium and the radiative capture by ^{171}Yb, ^{172}Yb, ^{173}Yb, ^{174}Yb and ^{176}Yb in the region up to 150 eV. The resonances were identified and their parameters determined for the first time. Strength function values were obtained for ^{171}Yb and ^{173}Yb: $S_o(171) = (1.1 \pm 0.4) \times 10^{-4}$; $S_o(173) = (2.4 \pm 0.9) \times 10^{-4}$. From the number of levels observed in ^{171}Yb and ^{173}Yb the authors estimated the σ parameter of the Bethe formula giving the level density as a function of the excitation energy and spin of the compound nucleus ($\sigma = 2.5$).

Table XIV

Resonance parameters of ytterbium isotopes

No.	E_o(eV)	Isotope	Γ(meV)	$g\Gamma_n$(meV)	$2g\Gamma_n^o$
1.	7.93±0.02	171		1.44±0.17	1.03±0.12
2.	8.13±0.02	171		0.49±0.06	0.34±0.04
3.	8.85±0.04	171		0.025±0.010	0.017±0.007
4.	13.13±0.07	171	93±10	2.5 ±0.1	1.38±0.06
5.	21.8 ±0.1	171		0.19±0.03	0.081±0.013
6.	28.2 ±0.1	171	70±10	1.8 ±0.1	0.68±0.04
7.	34.7 ±0.2	171		3.8 ±0.8	1.3 ±0.3
8.	41.5 ±0.2	171	168±70	7.2 ±0.7	2.2 ±0.2
9.	46.5 ±0.3	171		0.90±0.15	0.26±0.04
10.	53.2 ±0.3	171		5±1	1.4 ±0.3

No.	E_o(eV)	Isotope	Γ(meV)	$g\Gamma_n$(meV)	$2g\Gamma_n^o$
11.	54.4 ±0.3	171		16±3	4.3 ±0.8
12.	60.4 ±0.4	171	143±36	4.3 ±0.3	1.10±0.08
13.	65.0 ±0.4	171		7±1	1.74±0.25
14.	77.3 ±0.6	171		11±2	2.5 ±0.5
15.	82.6 ±0.6	171		2.4 ±0.3	0.53±0.07
16.	84.7 ±0.7	171		2.5 ±0.4	0.54±0.09
17.	96.1 ±0.8	171		3.0 ±0.4	0.61±0.08
18.	108±1	171		37±7	7.1 ±1.4
19.	113±1	171		14±3	2.6 ±0.5
20.	128±1.2	171		20±5	3.5 ±0.9
21.	141±1.4	171		10±2	1.7 ±0.3
22.	147±1.5	171		7±2	1.2 ±0.3
23.	4.53±0.01	173		0.082±0.009	0.007±0.008
24.	17.80±0.07	173	100±10	14±1	6.6 ±0.5
25.	31.6 ±0.15	173	165±14	36±3	12.8 ±1.1
26.	35.8 ±0.2	173		24±4	8.0 ±1.3
27.	45.5 ±0.2	173	104±16	15±1.4	4.4 ±0.4
28.	53.8 ±0.3	173		6.6 ±1.2	1.8 ±0.3
29.	59.0 ±0.4	173	141±65	4.0 ±0.7	1.0 ±0.2
30.	66.7 ±0.5	173	143±24	15.6 ±1.2	3.8 ±0.3
31.	69.1 ±0.5	173		5.3 ±0.7	1.3 ±0.2
32.	74.8 ±0.6	173		4.1 ±0.7	0.95±0.12
33.	76.7 ±0.6	173		18±3	4.1 ±0.7
34.	97.5 ±0.8	173		6.4 ±0.8	1.3 ±0.2
35.	106±1	173		26±5	5±1
36.	112±1	173		5.4 ±0.8	.1±0.2
37.	125±1.2	173		9.4 ±1.4	1.7 ±0.2
38.	130±1.2	173		13.6 ±1.8	2.4 ±0.3
39.	40.3 ±0.2	170	306±46	197±14	31±2
40.	73.2 ±0.5	170		77±12	9.0 ±1.4
41.	22.6 ±0.1				
42.	141±1.5	172			

DEPENDENCE OF THE DOPPLER BROADENING OF NEUTRON RESONANCES ON CHEMICAL BINDING; THE 405-eV RESONANCE IN ^{35}Cl

E.N. Karzhavina, A.B. Popov, I.I. Shelontsev
and Yu.S. Yazvitsky
JINR Preprint P-2198, Dubna, 1965

When resonance neutrons interact with atomic nuclei the change in the area beneath the resonance curve as a result of the Doppler effect may significantly influence the experimental results in cases when one is determining resonance parameters by analysing the areas under the resonance curves.

The authors studied the behaviour of the areas under the 405-eV resonance curve for ^{35}Cl as affected by the type of compound and the sample temperature.

Using the neutron spectrometer at the Joint Institute for Nuclear Research, they measured the transmission curves of three compounds of natural chlorine in which the atoms were linked with atoms of other elements of widely differing weight: NaCl, CCl_4, $PbCl_2$.

The thickness of ^{35}Cl in the samples was 2.075×10^{22} atoms/cm^2 $\pm$0.5%; this corresponded to the region of maximum Doppler corrections as a function of sample thickness.

The effect of sample temperature on the area beneath the resonance curve was studied with the NaCl and CCl_4 compounds. The transmission curves for the NaCl (thickness of $^{35}Cl = 2.13 \times 10^{22}$ atoms/cm^2) and CCl_4 (thickness of $^{35}Cl = 1.93 \times 10^{22}$ atoms/cm^2) samples were measured at 300°K and 77°K.

The results were as follows:

1. The difference between the areas beneath the 405-eV resonance curve of ^{35}Cl in the NaCl, CCl_4 and $PbCl_2$ compounds did not exceed the accuracy with which the areas were measured: 1.5%. (Fig 8)

2. When the NaCl sample was cooled to 77°K the area changed by 10 ± 0.3%; however, when the CCl_4 sample was cooled no change occurred. (Fig. 9)

From the transmission and self-indication curves values of 0.037 ± 0.002 eV and 0.82 ± 0.09 eV were obtained for $g\Gamma_n$ and Γ respectively for the 405-eV resonance of ^{35}Cl in samples with different thicknesses.

CALCULATION OF MULTIPLE INTERACTIONS FOR NEUTRON RADIATIVE CAPTURE EXPERIMENTS

F.F. Mikhailus, L.B. Pikelner and E.I. Sharapov
JINR Preprint P-2455, Dubna, 1965

One of the main obstacles to attaining exact values for neutron partial cross-sections is the effect of multiple interactions between neutrons and the nuclei in the sample. In the present work these interactions are calculated by means of the Monte Carlo method. A programme was written for the M-20 computer and corrections calculated for experiments on neutron scattering and neutron radiative capture and experiments involving self-indication.

Experimental verification for the case of radiative capture showed that the experimental and calculated results were in good agreement. They are in satisfactory agreement with the results of the approximate analytical calculation performed by Draper (Nucl. Sci. Eng. 1 (1956) 522) when the thicknesses of the samples are not too high and when $\Gamma_\gamma \gtrsim \Gamma_n$. In cases of high surface densities and for $\Gamma_\gamma \ll \Gamma_n$ the Draper method gives excessively low values for the correction.

ALPHA DECAY FROM HIGHLY EXCITED STATES IN SAMARIUM ISOTOPES

I. Kvitek and Yu.P. Popov
Paper to the XVI Annual Conference on Nuclear Spectroscopy and Structure of the Atomic Nucleus
Moscow, 1966

The authors investigated the probabilities of alpha transitions from excited states of ^{148}Sm and ^{150}Sm with different spins. The samarium nuclei were excited by means of resonance neutrons.

The lifetimes were found of the excited states with spins 3^- and 4^-. The measured probabilities of $4^- \rightarrow 2^+$ transitions in ^{150}Sm were found to

be in satisfactory agreement with the probabilities calculated on the basis of statistical theory.

Table XV shows the experimental results, including the alpha widths of the neutron resonances.

Table XV

Target nucleus	^{149}Sm				^{147}Sm								
E_o eV	0.098	0.88	5.0	17.1	3.4	18.3	29.8	32.1	39.9	49.4	58	83.5	183
I^π	4^-	4^-	4^-	-	3^-	4^-							
$\frac{\Gamma_\alpha}{\Gamma_\gamma} \times 10^6$	1.0±0.25	0.85±0.2	1.8±0.8	10±2.5	31±9	5±0.8	8±2	3±1	12±5	17±3	10±3	33±7	56±15
$\Gamma_\alpha \times 10^7$, eV	0.63	0.5	1.2	6.5	19	2.0	4.8	1.6	7	10	5.9	20	27
$\tau \times 10^9$, sec	10	12	5.2	1.0	0.3	3.1	1.3	3.9	0.9	0.6	1.1	0.3	0.23

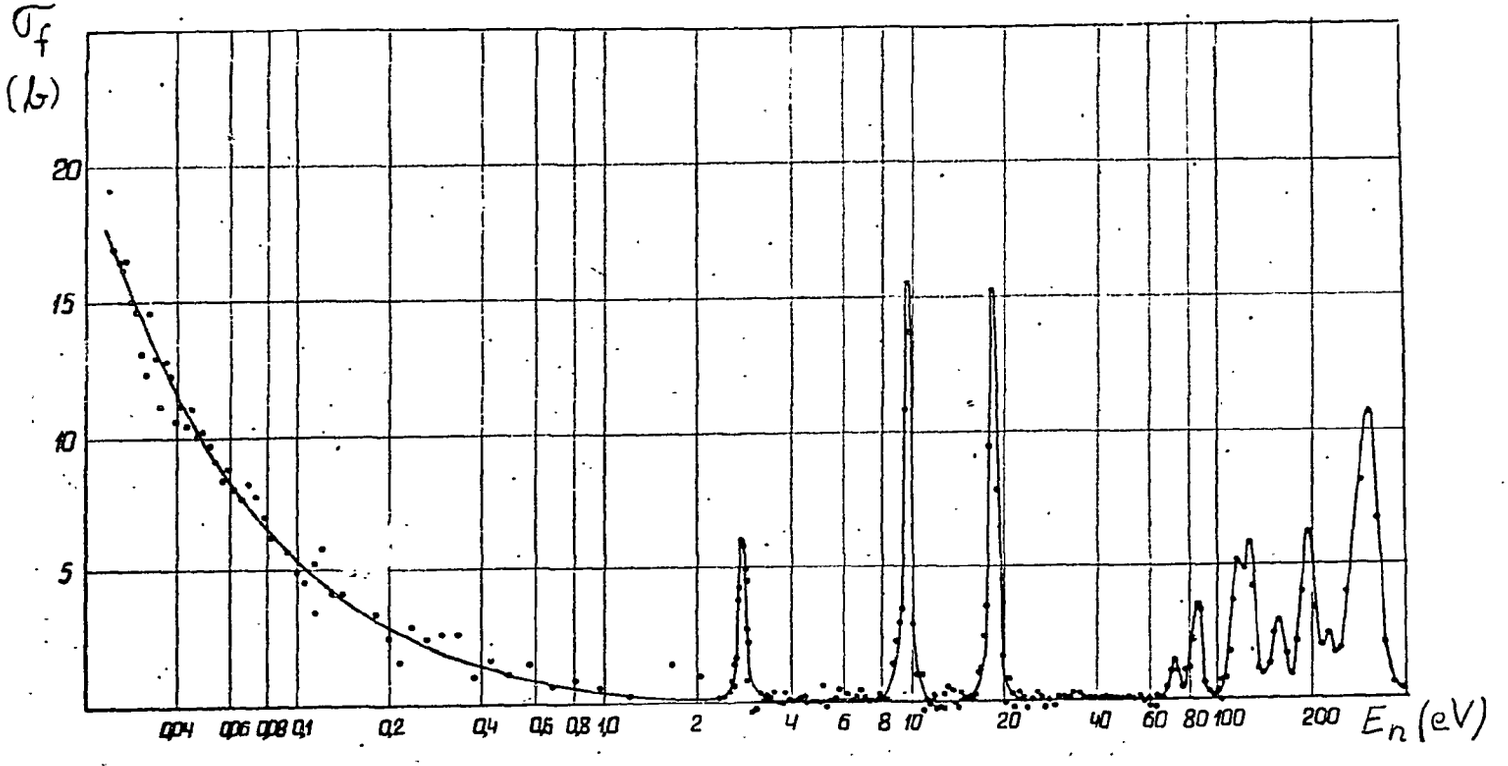

Fig. 2

Fission cross-section of ^{238}Pu

Fig. 1

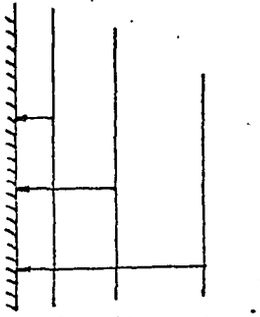

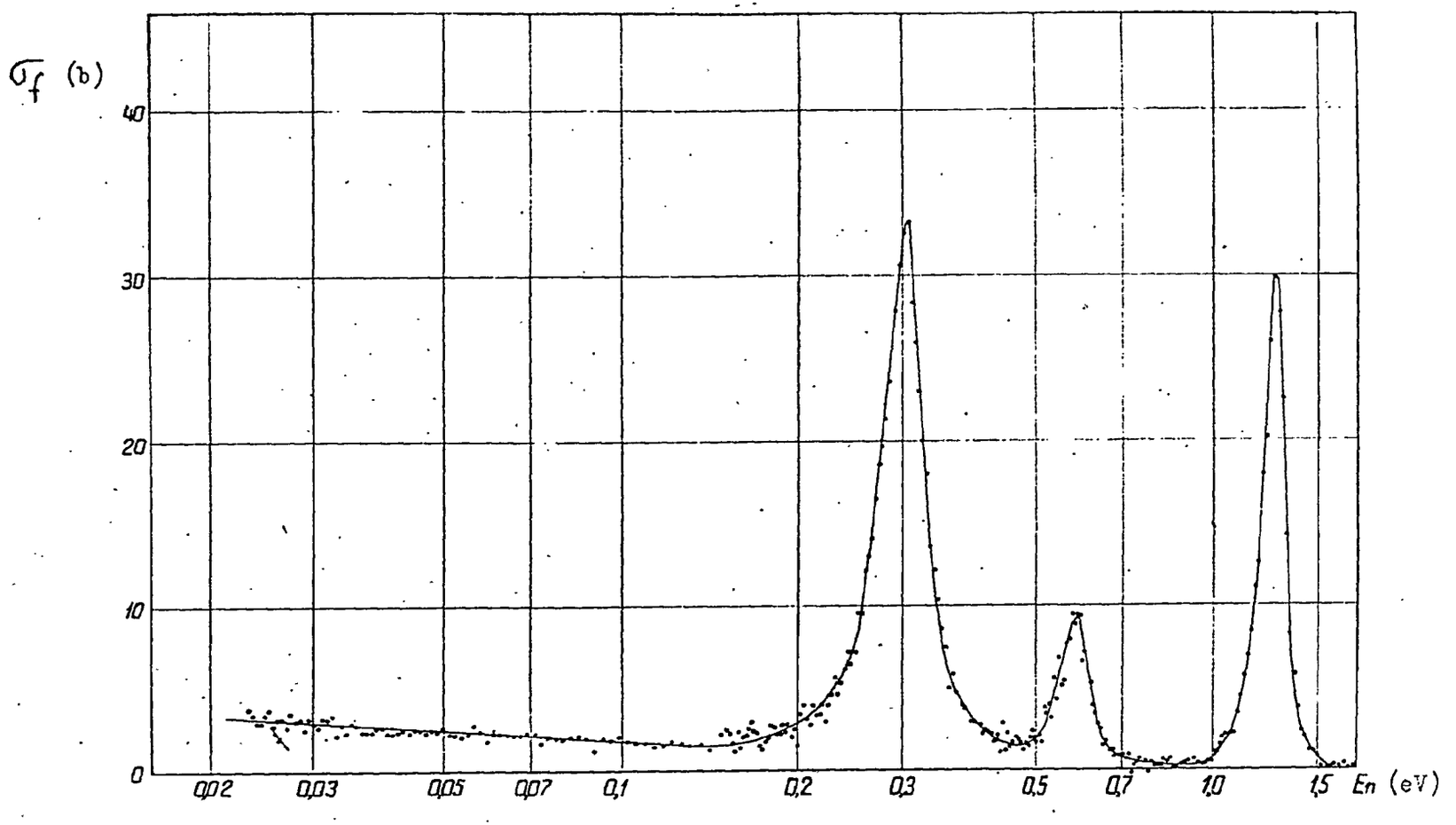

Fig. 3

Fission cross-section of ^{241}Am

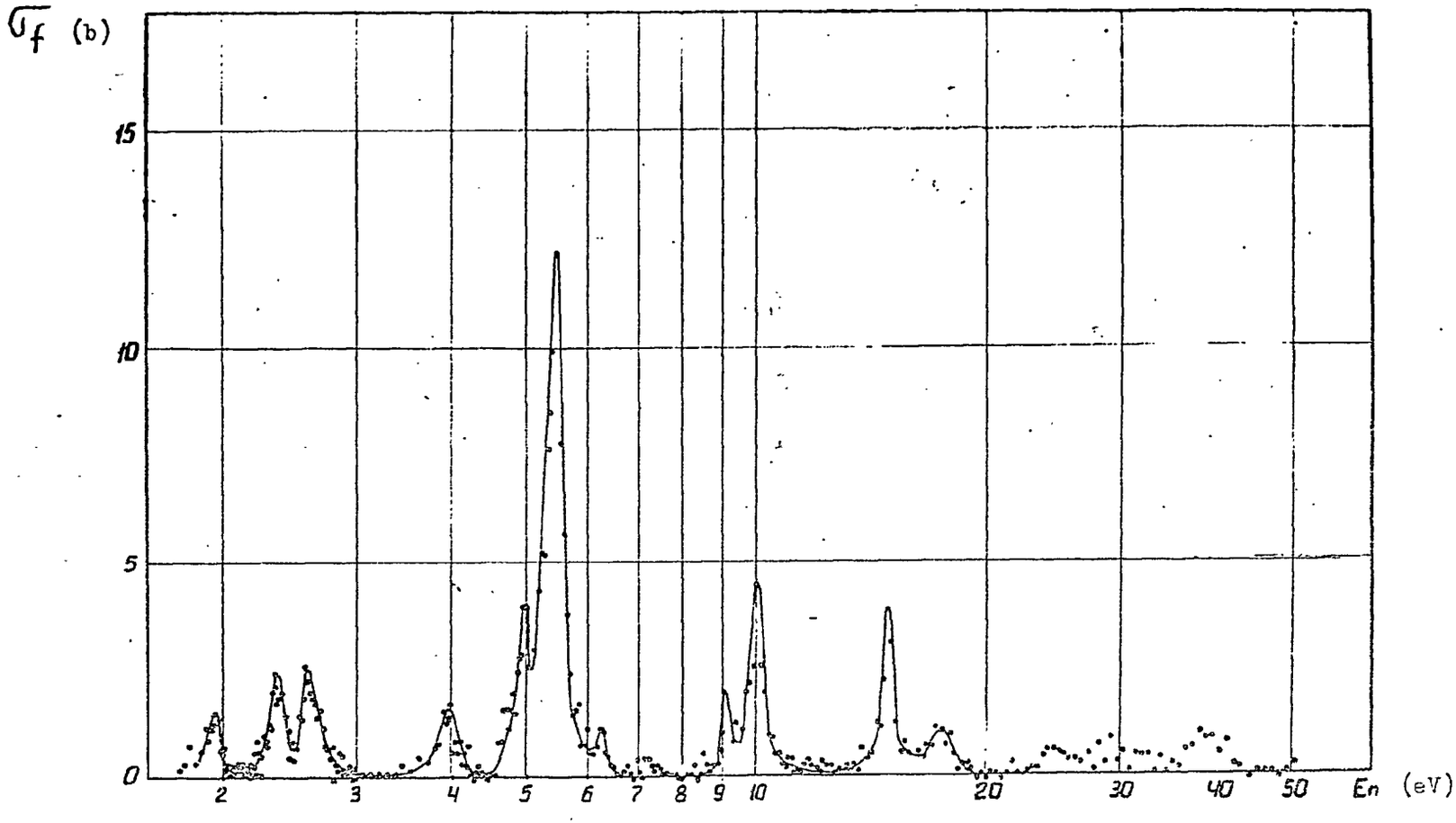

Fig. 4

Fission cross-section of ^{241}Am

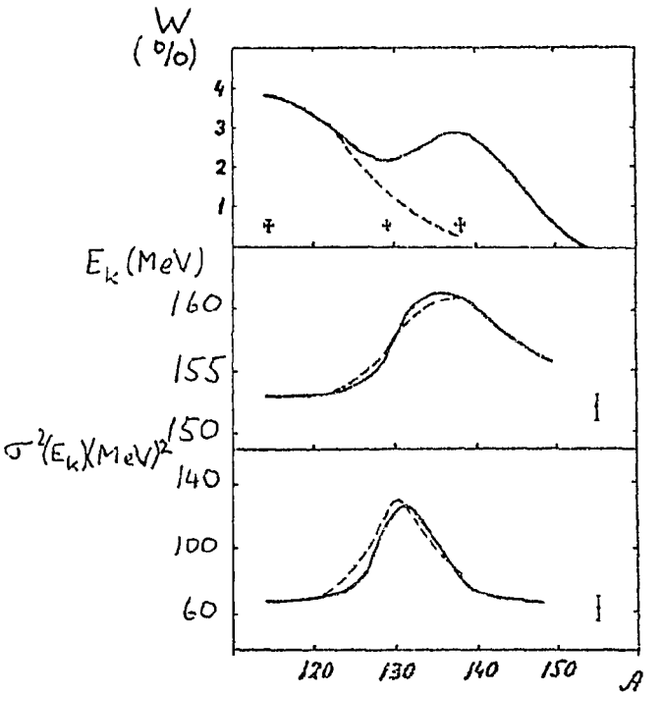
W
(%)
4
3
2
1
E_k (MeV)
160
155
150
140
100
60
$\sigma^2(E_k)$(MeV)^2
I
I
120
130
140
150
A

Fig. 5

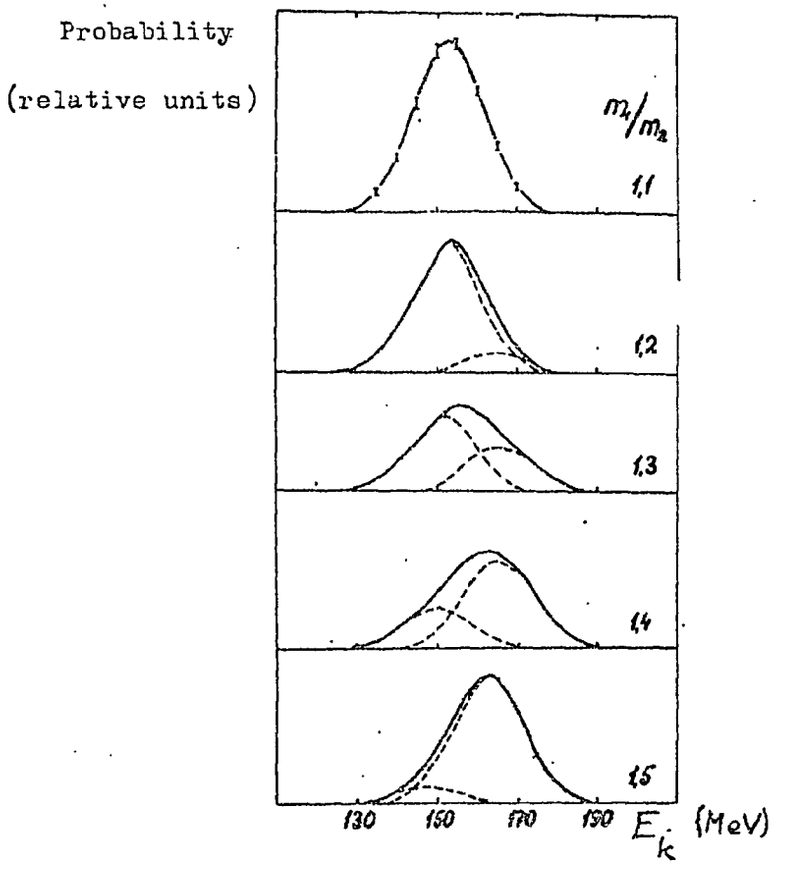
Probability
(relative units)
m_1/m_2
1,1
1,2
1,3
1,4
1,5
130
150
170
190
E_k (MeV)

Fig. 6

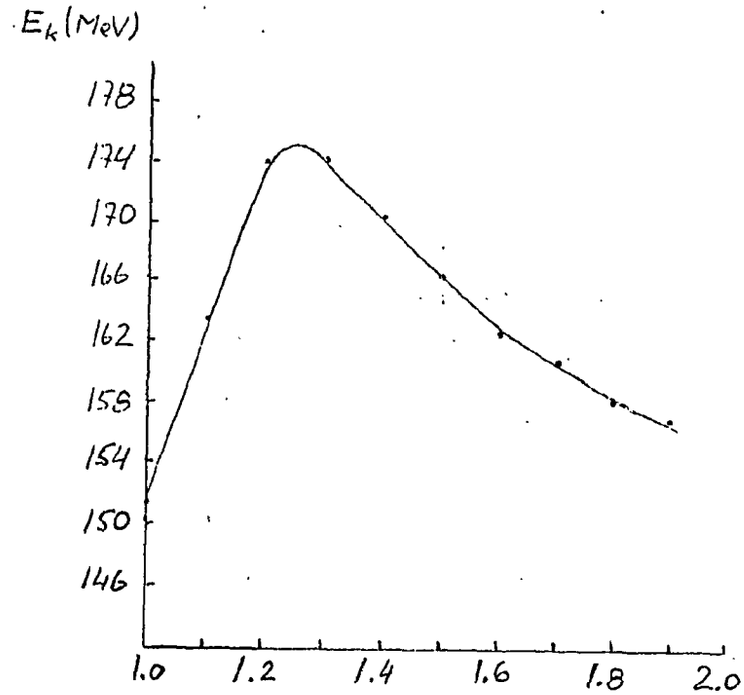

Fig. 7 Mass ratio of fragments, M(heavy)/M(light)

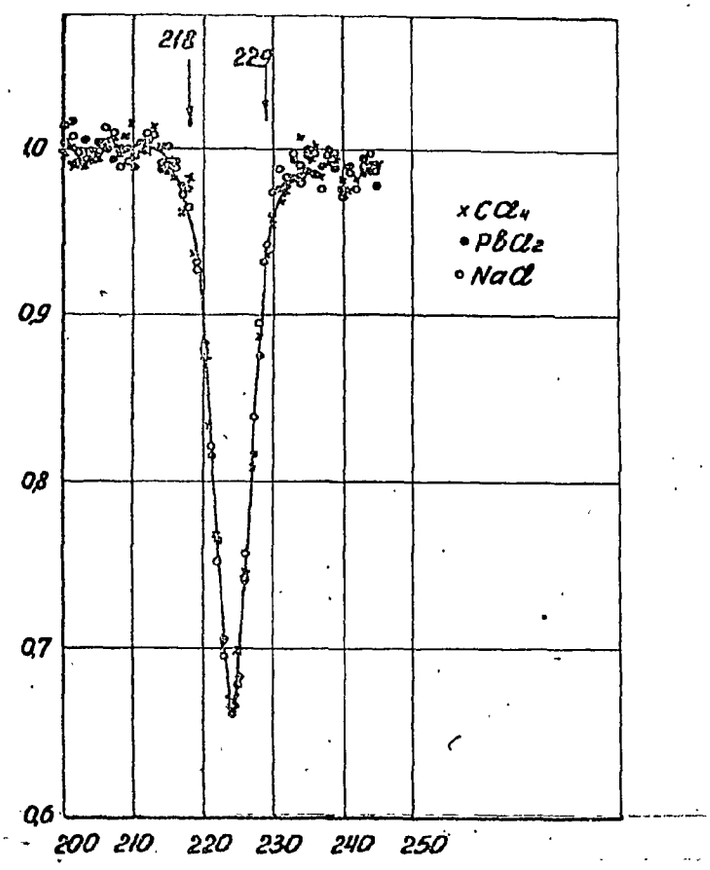

Fig. 8

The 405-eV resonance of ^{35}Cl in the compounds CCl_4, NaCl and $PbCl_2$ (thicknesses of ^{35}Cl = 2.075 x 10^{22} atoms/cm^2)

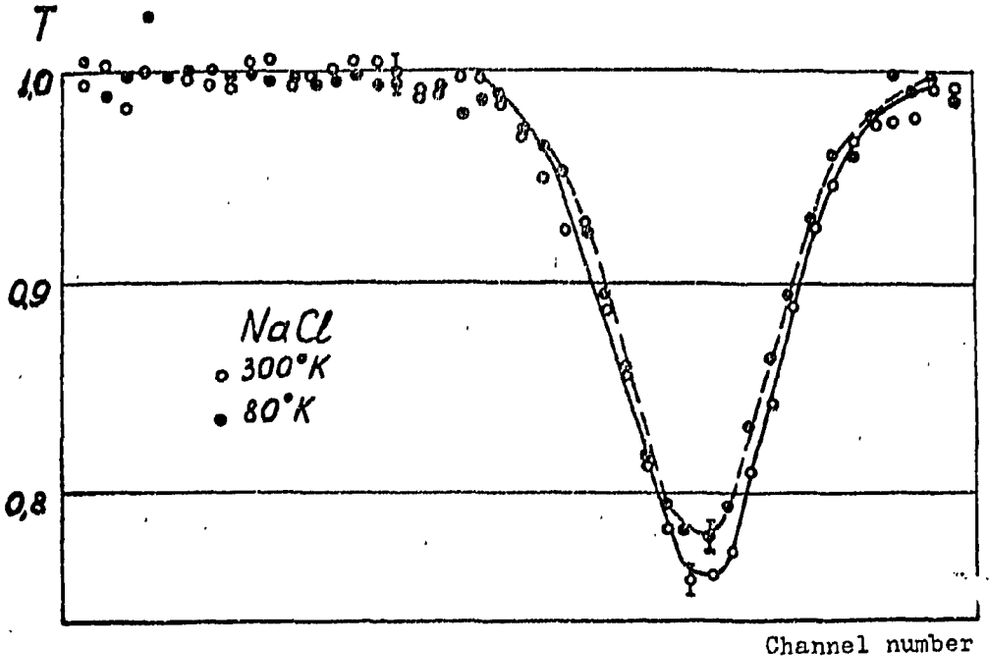

Fig. 9

The 405-eV resonance of ^{35}Cl in NaCl at 300°K and 77°K